

ORTHOGONAL GRIDS ON MEANDER-LIKE REGIONS*

MARIANELA LENTINI[†] AND MARCO PALUSZNY[‡]

Dedicated to Víctor Pereyra on the occasion of his 70th birthday

Abstract. Lemniscates are level curves of the absolute value of univariate complex polynomials. We consider the approximation of meander-like regions (i.e., regions similar to meandering rivers) by pairs of confocal lemniscates that are stitched together continuously. We look at orthogonal grids on these types of plane regions. The main application is in the area of numerical solution of partial differential equations.

Key words. lemniscate, orthogonal grid, path approximation

AMS subject classifications. 65L50, 65M50, 65N50

1. Preliminaries. The construction of grids on irregular regions has been mainly developed for use in numerically solving partial differential equations. To solve numerically a set of partial differential equations on a two dimensional region Ω , using finite differences, the main idea is to discretize the equations on a set of points, defined on the boundary and the interior of Ω where the properties of the phenomenon to be studied will be measured. The quality of the generated grid will impact the computational error in the numerical solution of the partial differential equations. Two factors are important: grid orthogonality and grid aspect ratios near to one. Both are required for the well conditioning of the discrete operator. In the literature, the most popular numerical procedures for generating a grid on Ω are conformal mapping methods, elliptic grid generation and variational methods.

A conformal mapping method produces a map from an orthogonally gridded region, like a rectangle, into the target region, which in the literature is referred to as physical space [16, 17]. Early discussions can be found in [4] and [8]. The conformality of the map, in theory, guarantees the orthogonality of the grid in the physical space; but in practice these methods may perform badly with respect to orthogonality and may perform well with respect to aspect ratios, since they are restricted to having the same scale factor in all directions. In the conformal mapping methods, the Schwarz-Christoffel transformations play a fundamental role [9]. Some drawbacks of these methods are documented in [15]. For a more thorough discussion of numerical conformal mappings between simply connected regions, see the interesting review paper [6]. The introduction of the covariant Laplace equations as a way to compute the grid points was proposed as a generalization of the idea of using a nonconstant scale factor in order to achieve orthogonality [15], but this led to the problem of getting some cells with very small scale factors.

Elliptic grid generation consists in solving an elliptic partial differential equation which enforces the orthogonality or near-orthogonality of the coordinate lines. For orthogonality, the Beltrami equations have to be solved [7]. These relax the more stringent conformality condition given by the Cauchy-Riemann equations. For near-orthogonality, Akcelik, et al. in [1] propose a further modification of the Beltrami system by introducing nonhomogeneous

* Received November 2, 2007. Accepted July 14, 2008. Published online on October 17, 2008. Recommended by Godela Scherer.

[†]Departamento de Ciencias Naturales y Matemáticas, Pontificia Universidad Javeriana. Cali, Colombia and Departamento de Cómputo Científico y Estadística, Universidad Simón Bolívar. Caracas, Venezuela. (mlentini@usb.ve).

[‡]Escuela de Matemáticas, Universidad Nacional, Sede Medellín. Medellín, Colombia and Laboratorio de Computación Gráfica y Geometría Aplicada, Universidad Central de Venezuela. Caracas, Venezuela. (mpalusznyk@unalmed.edu.co).

correction terms for the control of the aspect ratio of the grid. A recent paper of Bourchtein and Bourchtein [5] studies the consistency of the solution of the Beltrami equations with certain boundary conditions that might be naturally imposed in order to guarantee the orthogonality of the grid.

The main idea of the variational approach is as follows. Given a planar region Ω find a continuous transformation \bar{x} of the unit square B_2 into the region Ω where $\bar{x}(\xi, \eta) = (x(\xi, \eta), y(\xi, \eta))$. If a grid is defined on B_2 using \bar{x} we obtain a grid on Ω . To get a useful grid in the context of the numerical solution of partial differential equations, the transformation \bar{x} should be a homeomorphism. Moreover, it should transform the boundary of B_2 into the boundary of Ω .

To find the homeomorphism \bar{x} , the problem can be set in variational terms, and there are many possible choices of functionals. The appropriate selection of the functional will depend on the additional properties that the grid should satisfy. Given a functional, i.e. the Lagrangian L , the transformation \bar{x} is the solution of the minimization problem

$$\min \iint L(x_\xi, x_\eta, y_\xi, y_\eta) d\xi d\eta. \quad (1.1)$$

In [2] and [3], Barrera et al. give a very clear presentation of the construction of the discrete versions of the main possible choices for the functional. If L is twice continuously differentiable solving (1.1) is equivalent to solve the related Euler-Lagrange equations

$$\begin{aligned} \frac{d}{d\xi} \left(\frac{\partial L}{\partial x_\xi} \right) + \frac{d}{d\eta} \left(\frac{\partial L}{\partial x_\eta} \right) &= 0, \\ \frac{d}{d\xi} \left(\frac{\partial L}{\partial y_\xi} \right) + \frac{d}{d\eta} \left(\frac{\partial L}{\partial y_\eta} \right) &= 0, \end{aligned} \quad (1.2)$$

with the boundary constraint $\bar{x}(\partial B_2) = \partial\Omega$.

The existence and uniqueness of the solution of the boundary value problem (1.2) depends on L . When it has a unique solution it can be solved numerically. The degree of difficulty of this process depends on the properties of L .

Grid orthogonality is a desirable property for the convergence and stability of numerical partial differential equation solvers. Useful reviews of orthogonal and nearly orthogonal grids on two dimensional regions are [1], [2] and the references therein. In [2], it is stated that the problem of generating an orthogonal grid on an irregular region is not fully settled yet.

The goal of this paper is to introduce a new method for the automatic generation of orthogonal grids on elongated two dimensional regions. Previous work on orthogonal grids on elongated regions is [10]. We refer to these as meander-like regions because of their similarity to actual riverbeds.

In fact, the construction of grids on river channels is important in numerical simulations of sediment and pollutant transport which involve the numerical solution of the Navier-Stokes equations. See [19] and also [14] for a novel methodology using splines for the generation of grids to study computational fluid dynamics models of oil spills in rivers.

Our method is based on lemniscates of complex polynomials and it guarantees automatically the orthogonality of the grid. We propose to “tile” the meander-like region with lemniscatic sectors. A lemniscatic sector is the region bounded by two confocal lemniscates and two arcs; the latter are orthogonal to the lemniscates. The two continuous curves given by joining corresponding lemniscatic segments of contiguous lemniscatic sectors approximate the two riverbeds of the meander-like region. Any two neighbouring lemniscatic sectors meet, within a given tolerance, along a common arc. The optimization required by the proposed method can be dealt with using standard routines of MATLAB.

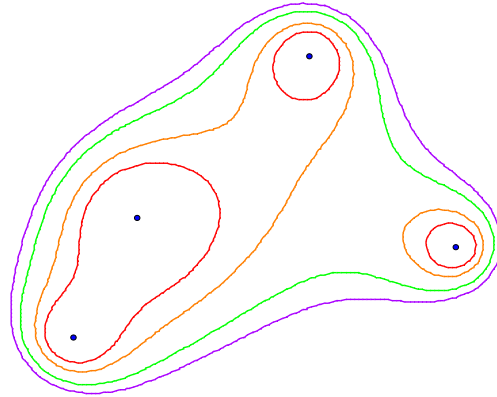


FIGURE 2.1. *Confocal lemniscates with four foci.*

2. Lemniscates, lemniscatic regions and grids. Given a polynomial $F(z) = (z - a_1)(z - a_2)\dots(z - a_n)$ and $\rho > 0$, we will refer to the level curve $\{z : |F(z)| = \rho\}$ as the lemniscate of radius ρ and foci a_1, a_2, \dots, a_n . Two lemniscates are confocal if they have the same foci. Lemniscates are bounded closed curves and confocal lemniscates are nested; see Figure 2.1. Good references for lemniscates are the beautifully written complex variables book of T. Needham [13] and the classical work [11].

The main goal of this paper is to offer a new look at an amply researched and very important problem: automatic generation of an orthogonal grid on a plane region.

The regions we deal with are the meander-like regions; see Section 4 for a full description. Other applications are in the areas of texture recording and data compression.

A lemniscatic region is the set of points between two confocal lemniscates. That is, a complex polynomial $F(z)$ and two positive numbers, $\rho_1 < \rho_2$, determine the lemniscatic region $\{z : \rho_1 < |F(z)| < \rho_2\}$. Lemniscatic regions might be disconnected sets. If we look

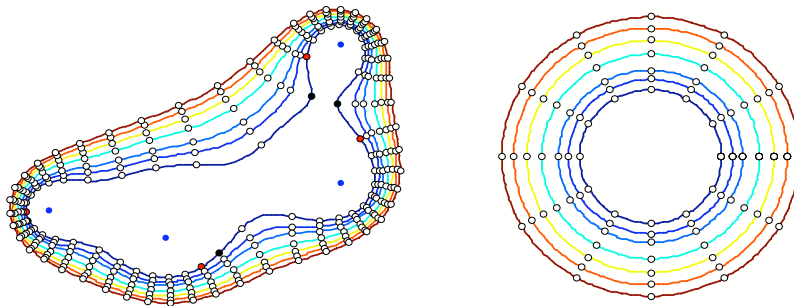


FIGURE 2.2. *Lemniscates and pre-images.*

at F as a mapping of the z -plane into the w -plane, it sends the lemniscates of F into circles centered at the origin. The radius of a lemniscate coincides with the radius of the circle it maps into.

If the region $\{z : \rho_1 < |F(z)| < \rho_2\}$ does not contain any zeros of the derivative of F then the map F is an $n : 1$ local homeomorphism (in the sense of covering spaces [12]). Figure 2.2 illustrates a lemniscatic region that does not contain any zeros of the derivative of a degree four polynomial F . The points in the lemniscatic region are the roots of the equation $F(z) - w = 0$, as w runs through points in the annulus, as shown in Figure 2.2. F is a

conformal mapping of the lemniscatic region into the annulus, i.e., it preserves angles, hence it maps orthogonal grids into orthogonal grids. Since it is trivial to produce orthogonal grids in an annulus and mapping them back to a lemniscatic region entails only finding roots of polynomials, this is an easy method to produce orthogonal grids on lemniscatic regions.

We will be mainly interested in sections of lemniscatic regions, namely subsets bounded by two confocal lemniscates and the inverse images of two radial segments of the annulus. We refer to the latter as rays of the lemniscatic region.¹ The grid on a section is now clear: it consists of the intersection points of intermediate lemniscates and the rays of the lemniscatic region. See Figure 2.2. Figure 2.3 shows the orthogonal grid on a section of a lemniscatic

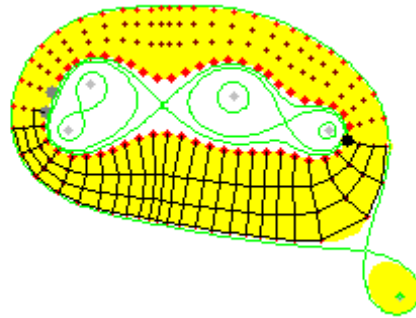


FIGURE 2.3. Section of lemniscatic region of a polynomial of degree 5.

region which consists of two connected components. The self-intersecting curves are singular lemniscates, i.e., lemniscates that pass through zeros of the derivative of the polynomial.



FIGURE 3.1. Air view of the Sacramento river and data points on its riversides.

3. Approximating meander-like regions. A meander-like region is an elongated region with identifiable length and varying width. Figure 3.1 shows the motivating picture for the definition. Other examples are brush traces, two dimensional images of curvilinear inner

¹The rays of the lemniscatic regions should not be confused with the rays of the annulus, the former are the inverse images of the latter under the polynomial mapping F .

body structures such as respiratory and digestive tracts. Very recently, meander-like regions surfaced in the computer aided geometric design setting as “fat conics” [18].

Given two sets of data points, one on each side of a riverbed, we would like to find a polynomial F and two positive radii ρ_1 and ρ_2 such that the lemniscates $\{z : |F(z)| = \rho_1\}$ and $\{z : |F(z)| = \rho_2\}$ approximate these two data sets. In the final section of this paper, we will comment on how to extend the sampling sets on both sides to cover the full riverbed. For

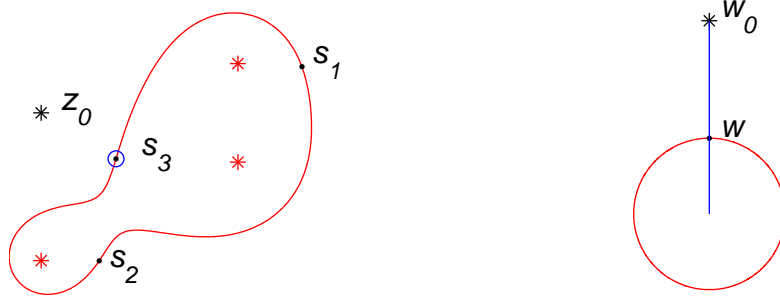


FIGURE 3.2. Computation of the distance between a lemniscate and a point z_0 looking at the roots of a polynomial.

the rest of this section we will look at the problem of approximating a portion of the riverbed with a lemniscatic region.

The approximation involves minimizing a continuous cost function, $H(a_1, a_2, \dots, a_n)$ where the a_i are the foci of the sought-after pair of confocal lemniscates. The function H depends on the distances of the points in DAT1 and DAT2 to the curves $\{z : |F(z)| = \rho_1\}$ and $\{z : |F(z)| = \rho_2\}$ respectively.

Given a point z_0 and a lemniscate $\Lambda = \{z : |F(z)| = \rho\}$, let s_1, s_2, \dots, s_n be the roots of the polynomial $F(z) - \rho e^{i\phi}$, where $0 \leq \phi < 2\pi$ is the argument of $F(z_0)$. We estimate the distance between the point z_0 and the lemniscate Λ as $\min(|z_0 - s_i|)$.

Figure 3.2 shows a lemniscate of radius ρ and foci a_1, a_2, a_3 and a point z_0 in the exterior and its image point $w_0 = F(z_0) = (z_0 - a_1)(z_0 - a_2)(z_0 - a_3) = \rho_0 e^{i\phi}$. The distance between z_0 and the lemniscate is the minimum of $|z_0 - s_1|$, $|z_0 - s_2|$ and $|z_0 - s_3|$ where s_1, s_2 and s_3 are the roots of $F(z) - \rho e^{i\phi}$. To find the monic polynomial and two positive numbers ρ_1 and ρ_2 as above we proceed as follows. For any given set of n complex numbers a_1, a_2, \dots, a_n , the foci of the lemniscates, we define the radii of the confocal lemniscates as

$$\rho_1 = \sqrt{\frac{1}{n_1} \sum_{z \in \text{DAT1}} |F(z)|^2}$$

and

$$\rho_2 = \sqrt{\frac{1}{n_2} \sum_{z \in \text{DAT2}} |F(z)|^2}$$

where n_1 and n_2 are the numbers of data points in DAT1 and DAT2, respectively. We define the cost function $H(a_1, a_2, \dots, a_n)$ as

$$\frac{1}{(n_1 + n_2)^2} \left(\sum_{u \in \text{DAT1}} F_u(a_1, a_2, \dots, a_n) + \sum_{u \in \text{DAT2}} F_u(a_1, a_2, \dots, a_n) \right)$$



FIGURE 3.3. Data sets DAT1 and DAT2 on the two sides of the Sacramento river.

where $F_u(a_1, a_2, \dots, a_n)$ is the square of the distance estimate between a point u and the lemniscate given by ρ_1 for $u \in \text{DAT1}$ and ρ_2 for $u \in \text{DAT2}$. The factor containing n_1 and n_2 , allows us to compare lemniscatic approximations when the number of sample points vary. The objective is then to minimize the cost function, i.e., to find the foci which make the cost minimum.

When DAT1 and DAT2 extend along long pieces of the riverbeds, as shown in Figure 3.3, the approximation task might require a pair of lemniscates with a large number of foci. Hence, the complex polynomial one has to deal with might have a high degree. This is inconvenient for numerical computations. To avoid working with high degree polynomials, DAT1 and DAT2 are partitioned into data subsets that face each other, and for each data subset pair we determine a complex cubic polynomial² and two positive numbers ρ_1 and ρ_2 such that each lemniscate approximates within a given tolerance each of the data subsets of the chosen pair. Figures 3.4 and 3.5 show data subsets pairs and the approximating confocal lemniscates.

4. Joining lemniscatic regions. As discussed in Section 3, within certain constraints we may construct an orthogonal grid on the region between two lemniscates by mapping back an orthogonal grid given in the annulus determined by two concentric circles. Moreover, as illustrated in Figure 2.2, the lemniscatic region determined by two segments of confocal lemniscates which face each other corresponds to a section of annulus. The latter is given by two concentric circular arcs which face each other. More precisely, a sector of the circular annulus cut off by two radial segments corresponds to the lemniscatic region which is bounded by the two lemniscatic segments and the two lemniscatic rays.³ The complex polynomial which maps the confocal lemniscates into concentric circles, as illustrated in Figure 2.2, is a one-to-one conformal map between the lemniscatic region and the sector of the annulus.

The partition of DAT1 and DAT2 into subsets which face each other (such that one subset of each pair is contained in DAT1 and the other in DAT2) has to be chosen so that the region determined by each data subset pair can be fitted with a lemniscatic region. Moreover, we

²Our computational experiments strongly suggest that it is always possible to partition DAT1 and DAT2 such that each data subset pair can be approximated, within a given tolerance, with lemniscates of cubic polynomials.

³A lemniscatic ray is a curve segment in the z -plane, i.e., the plane where the lemniscates live or, equivalently, the physical space, which is mapped into a radial segment of the circular annulus.

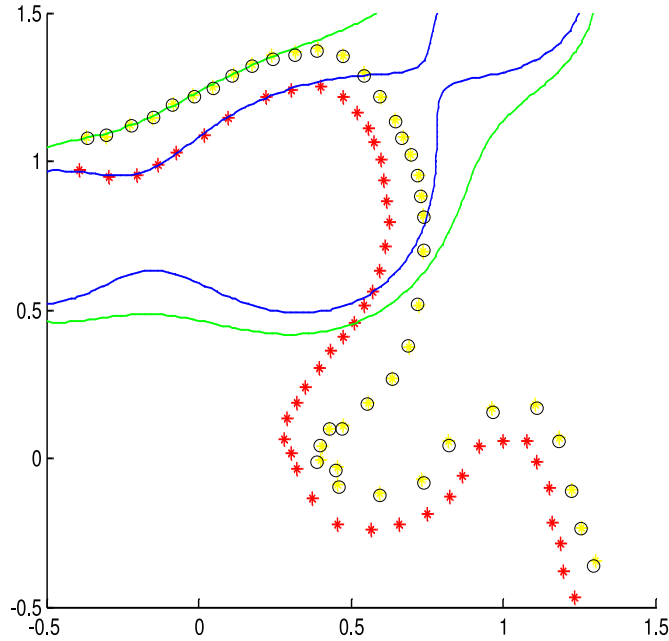


FIGURE 3.4. *Lemniscate pair approximating the first subsets of DAT1 and DAT2.*

have to guarantee that the lemniscatic region corresponding to two contiguous data subsets meet along a lemniscatic ray of each one of the lemniscatic regions. See Figure 4.1.

Our algorithm offers fully automatic partitioning of the input DAT1 and DAT2. The only required user input is a tolerance for the data approximation and a target number for the number of sectors that should compose the complete meander-like region. A slightly modified version of the above cost function is used to enforce the condition that the lemniscatic regions meet along lemniscatic rays within the given tolerance. This modification consists of adding a penalty term when lemniscatic rays of neighboring lemniscatic sectors do not coincide. Our numerical experiments suggest that it is enough to impose a penalty on the euclidean distance between the two endpoints of the last ray of one sector and the two endpoints of the first ray of the next sector.

5. The orthogonal grid and examples. As explained in Section 2, the generation of the grid reduces to solving cubic equations. Although it is well known that polynomial root finding might be numerically unstable in the neighborhood of a multiple root, this does not affect our method because we stay away from zeros of the derivative of $F(z)$: the approximating polynomial $F(z)$ is chosen so that the lemniscatic region given by ρ_1 and ρ_2 does not contain singularities.

We illustrate the resulting grids obtained from five runs of our system for the data set DAT1 and DAT2 for the boundaries of the Sacramento river. There are 40 data points on the right riverside and 47 points on the left. Our algorithm starts with three random foci to determine each pair of confocal lemniscates. Figure 5.1 illustrates the pairs of confocal lemniscates that approximate each pair of data subsets, and Figure 5.2 shows the resulting grid. The data set was subdivided into nine pairs of data subsets. Figures 5.3, 5.4, 5.5 and 5.6 depict four additional grids for the same data set, also using nine pairs of data subsets. Ta-

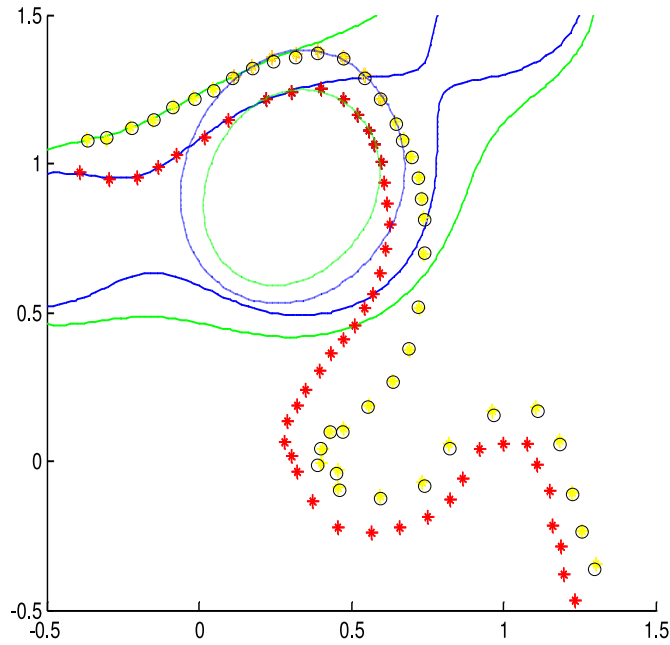


FIGURE 3.5. Lemniscate pair approximating the second subsets of data on the sides of the riverbed together with those of the first subsets.

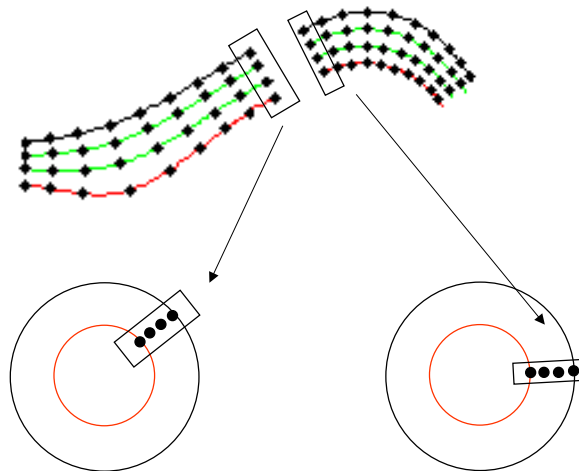


FIGURE 4.1. Common lemniscatic ray between contiguous lemniscatic regions .

ble 5.1 summarizes the information regarding the number of cells, the average aspect ratio (AAR), the maximum aspect ratio (MAR), the average deviation of orthogonality (ADO) and the maximum deviation of orthogonality (MDO), the latter two were computed using angles.

As mentioned above, the grid examples in this section correspond to the same data set and the number of sections is nine for each case. We believe that this feature is an advantage, since it hands to the user (or to an automatic procedure) a number of grid options which can

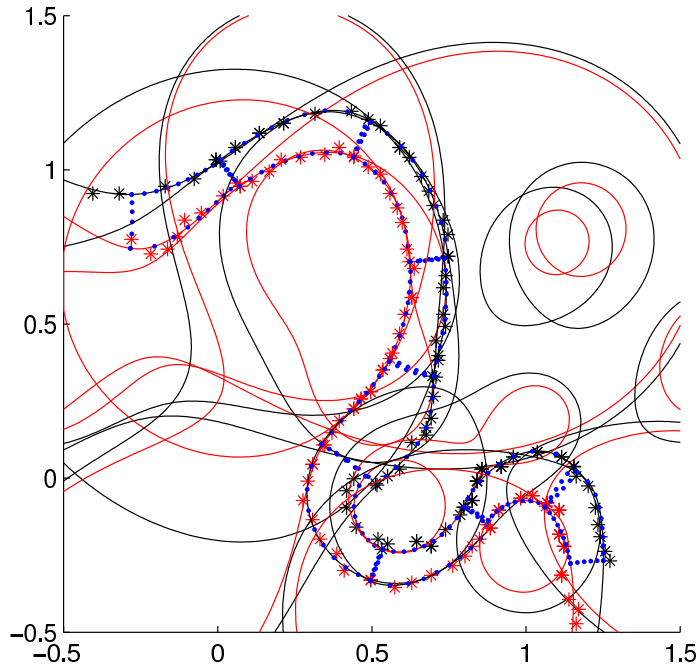


FIGURE 5.1. Nine pairs of confocal approximating lemniscates.

TABLE 5.1

Statistics over five trials of the grid generator for the Sacramento river data corresponding to Figures 5.2, 5.3, 5.4, 5.5 and 5.6.

Figure	AAR	MAR	ADO	MDO	Cell Number
5.2	1.3339	2.2832	0.0288	0.3444	572
5.3	1.5048	3.9196	0.0304	0.2639	650
5.4	1.4484	2.5485	0.0306	0.6156	626
5.5	1.4845	3.3662	0.0360	0.5693	590
5.6	1.2979	2.4151	0.0304	0.2446	553

be compared/validated in the context of the use for which the grid is intended. The reason why this is possible stems from the fact that the algorithm starts with a random choice of three foci for the first pair of lemniscates which approximate the first data subset pair.

6. Conclusions. We introduce a new method for the automatic generation of orthogonal grids on meander-like regions. The method depends only on root finding of cubic complex polynomials and the minimization of a cost function. The algorithm automatically partitions the data on both boundaries of the meander-like region, and approximates each pair of data subsets that face each other by segments of confocal lemniscates. The lemniscatic regions given by pairs of confocal lemniscates and lemniscatic rays tile the meander-like region.

The only input required from the user is the tolerance for the approximation and the maximum number of regions. The algorithm uses the standard optimization routine `lsqnonlin` of the MATLAB system.

A comparison with other methods is undertaken by computing the maximum and average deviation of orthogonality (MDO and ADO) and the maximum and average aspect ratios (MAR and AAR) of the grids. The MAR, AAR, MDO and ADO are computed for the concrete example of the Sacramento river.

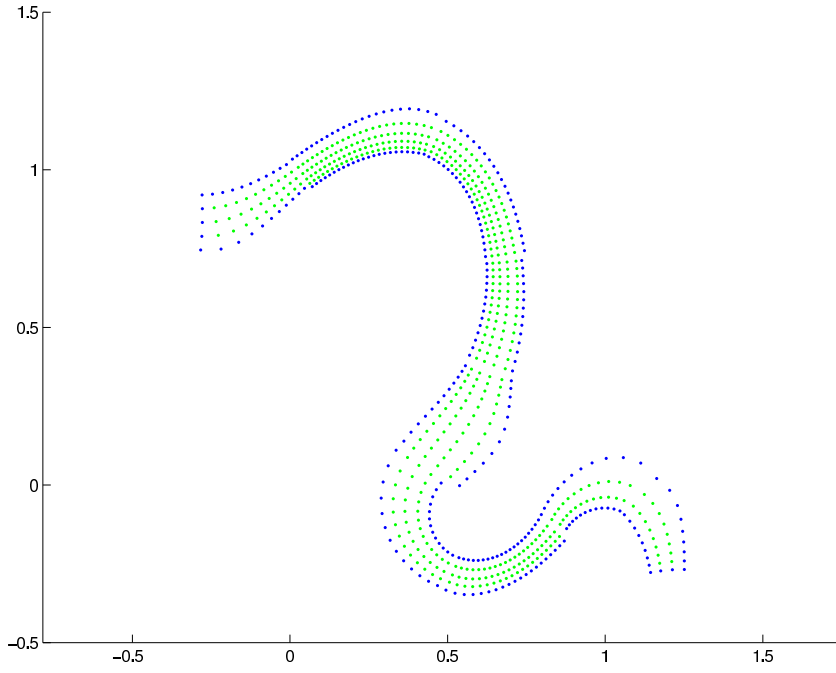


FIGURE 5.2. Grid corresponding to the lemniscates of Figure 5.1.

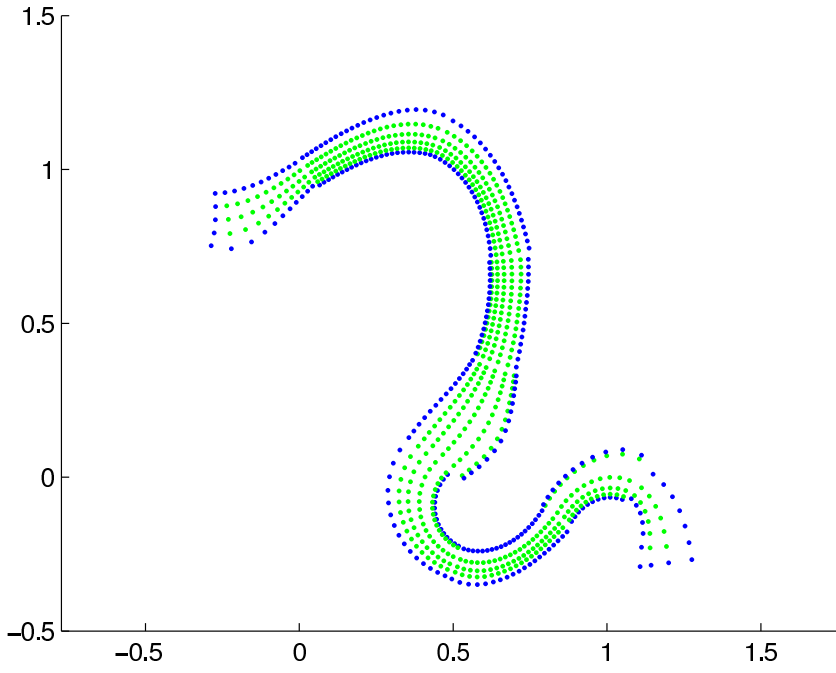


FIGURE 5.3. Second grid for the Sacramento river data.

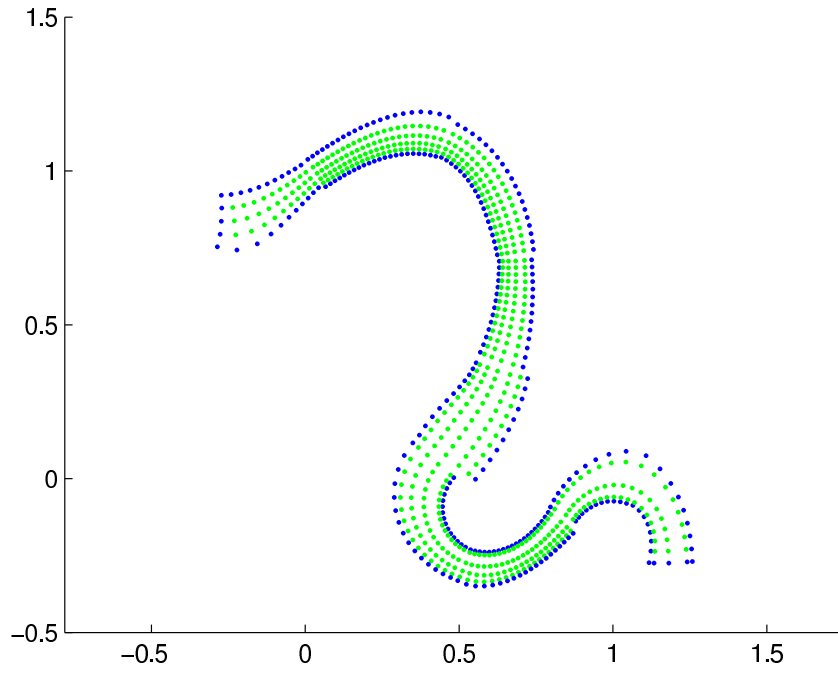


FIGURE 5.4. *Third grid for the Sacramento river data.*

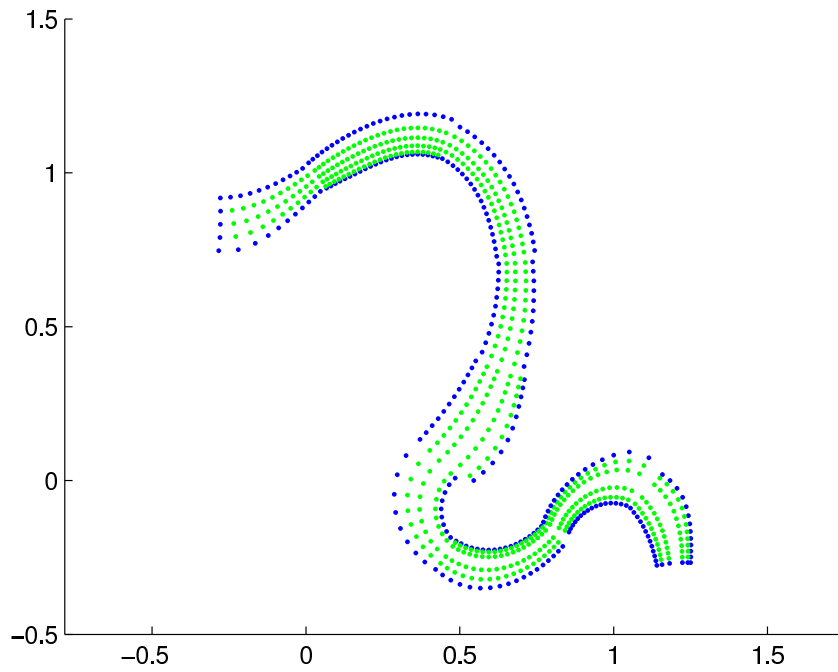


FIGURE 5.5. *Fourth grid for the Sacramento river data.*

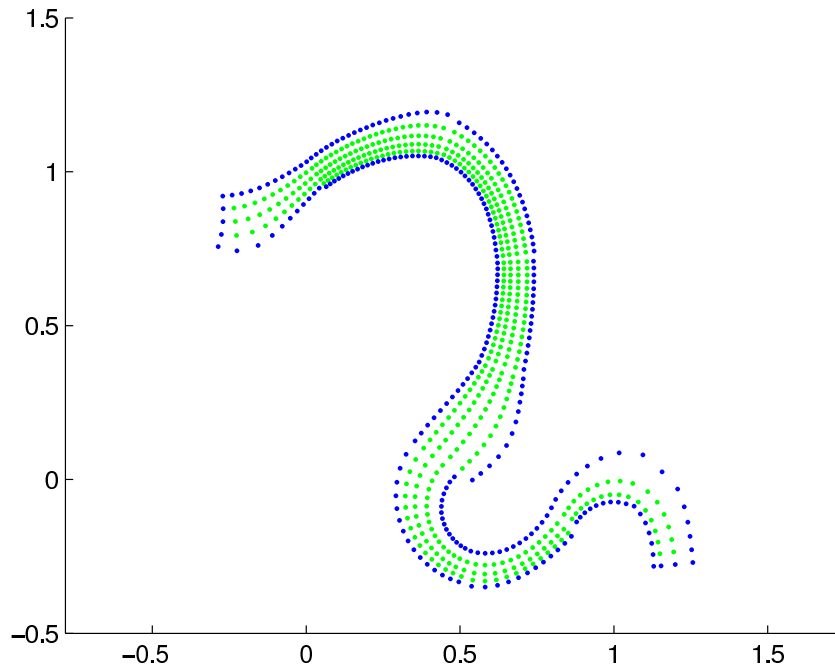


FIGURE 5.6. *Fifth grid for the Sacramento river data.*

Acknowledgments. The authors are thankful to the referees for their thorough comments, which substantially improved the paper.

REFERENCES

- [1] V. AKCELIK, B. JARAMAZ, AND O. GHATTAS, *Nearly orthogonal two-dimensional grid generation with aspect ratio control*, J. Computational Phys., 171 (2001), pp. 805–821.
- [2] P. BARRERA-SÁNCHEZ, F. J. DOMÍNGUEZ-MOTA AND G. F. GONZÁLEZ FLORES, *Una revisión de los funcionales de área*. <http://www.matematicas.unam.mx/pablo/>, 2004.
- [3] P. BARRERA-SÁNCHEZ, G. F. GONZÁLEZ FLORES AND F. J. DOMÍNGUEZ-MOTA, *Some experiences on orthogonal grid generation*, Appl. Numer. Math., 40 (2002), pp. 179–190.
- [4] L. BIEBERBACH, *Conformal Mapping*, Chelsea, New York, fourth ed., 1964.
- [5] A. BOURCHTEIN AND L. BOURCHTEIN, *On generation of orthogonal grids*, Appl. Math. Comput., 173 (2006), pp. 767–781.
- [6] T. K. DELILLO, *The accuracy of numerical conformal mapping methods: a survey of examples and results*, SIAM J. Numer. Anal., 31 (1994), pp. 788–812.
- [7] L. ECA, *2D orthogonal grid generation with boundary point distribution control*, J. Computational Phys., 125 (1996), pp. 440–453.
- [8] P. HENRICI, *Applied and Computational Complex Analysis*, Wiley, New York, 1974.
- [9] L. HILL HOWELL, *Computatation of conformal maps by modified Schwarz-Christoffel transformations*, PhD thesis, MIT, 1990.
- [10] C. HU, *Algorithm 785: a software package for computing Schwarz-Christoffel conformal transformations for doubly connected polygonal regions*, ACM Trans. Math. Software, 24 (1998), pp. 317–333.
- [11] A. I. MARKUSHEVICH, *Theory of functions of a complex variable*, Chelsea, second ed., 1985. Translated from Russian.
- [12] J. R. MUNKRES, *Topology*, Prentice Hall, second ed., 1999.
- [13] T. NEEDHAM, *Visual Complex Analysis*, Clarendon Press, Oxford, 1998.
- [14] B. A. SOUZA, E. M. MATOS, L. T. FURLAN, AND J. R. NUNHEZ, *A simple method for orthogonal and nonorthogonal grid generation*, Computers and Chemical Engineering, 31 (2007), pp. 800–807.
- [15] G. RYSKIN AND L. G. LEAL, *Orthogonal mapping*, J. Computational Phys., 50 (1983), pp. 71–100.
- [16] J. F. THOMPSON, Z. U. A. WARSJ AND W. MASTIN, *Numerical Grid Generation*, Elsevier Science Pub-

- lishers, 1985.
- [17] http://www.cfd-online.com/Wiki/Structured_mesh_generation.
- [18] X. YANG AND W. YANG, *Cone spline approximation via fat conic spline fitting*, Computer-Aided Design, 38 (2006), pp. 703–712.
- [19] Y. ZHANG AND Y. JIA, *CCHE2D mesh generator and user manual (v 2.00)*, Technical Report NCCHE-TR-2002-5, National Center for Computational Hydroscience and Engineering, School of Engineering, University of Mississippi, 2002.